

LINDA HALL LIBRARY

5109 CHERRY STREET
KANSAS CITY, MISSOURI
64110-2498

PHONE

(816) 363-4600

FAX:

(816) 926-8785



EC

2/7/12 DocServ #: 663397

16:29

SHIP TO:

016659

Attn: Jan Killian

Stress Engineering Services, Inc.

13800 Westfair East Drive

Houston TX 77041

US

Shelved as:

Location:

Title: Journal of Tribology

Volume: 117

Issue: 1

Date: January 1995

Author: C.R. Alexander, D.W. Childs, Z. Yang

Article Title: Theory versus Experiment for the
Rotordynamic Characteristics of a Smooth
Annular Gas Seal at Eccentric Positions

Pages:

148-152 (5)

Accept Non English? No

Fax: 281-955-2638

Phone: 281-955-2900

Ariel:

Email: jan.killian@stress.com

Regular

ElecDel

LHL

SupplierWillPay

Max Cost: 100.00

Reference Number: 9110214CRA

Account Number:

FEDEX Account Number:

Notes:

asm 7/PL
©6.00

DOCserv / WEB / PULL SLIP

Theory Versus Experiment for the Rotordynamic Characteristics of a Smooth Annular Gas Seal at Eccentric Positions¹

C. R. Alexander

Stress Engineering Services, Inc.,
Houston, TX 77041-1101

D. W. Childs

Turbomachinery Laboratory,
Texas A&M University,
College Station, TX 77843-3123

Z. Yang

Cummins Engine Co., Inc.,
Fuel Systems,
Charleston, SC

Experimental results are presented for the rotordynamic coefficients of a smooth gas seal at eccentricity ratios out to 0.5. The effects of speed, inlet pressure, pressure ratio, fluid prerotation, and eccentricity are investigated. The experimental results show that direct stiffness K_{XX} decreases significantly, while direct damping and cross-coupled stiffness increase with increasing eccentricity. The whirl-frequency ratio, which is a measure of rotordynamic instability, increases with increasing eccentricity at 5000 rpm with fluid prerotation. At 16,000 rpm, the whirl-frequency ratio is insensitive to changes in the eccentricity. Hence, the results show that eccentric operation of a gas seal tends to destabilize a rotor operating at low speeds with preswirl flow. At higher speeds, eccentric operation has no significant impact on rotordynamic stability. The test results show that the customary, eccentricity-independent, model for rotordynamic coefficients is only valid out to an eccentricity ratio of 0.2~0.3. For larger eccentricity ratios, the dependency of rotordynamic coefficients on the static eccentricity ratio needs to be accounted for. Experimental results are compared to predictions for static and dynamic characteristics based on an analysis by Yang (1993). In general, the theoretical results reasonably predict these results; however, theory overpredicts direct stiffness, fails to indicate the decrease in K_{XX} that occurs with increasing eccentricity, and incorrectly predicts the direction of change in K_{XX} with changing pressure ratio. Also, direct damping is substantially underpredicted for low preswirl values and low supply pressures, but the predictions improve as either of these parameters increase.

Introduction

Annular pressure seals are installed in turbomachinery to limit the leakage of a fluid between adjacent regions at different pressures. To increase performance, design trends have developed machinery with higher speeds and tighter clearances which can produce unstable subsynchronous, whirling motion. Annular gas seals are known to provide destabilizing mechanisms for high-performance turbomachinery, Childs (1993).

Two linearized models have been developed for the reaction force developed by an annular gas seal. The first model is for small motion about a centered position within a gas seal and is expressed

$$-\begin{Bmatrix} F_X \\ F_Y \end{Bmatrix} = \begin{bmatrix} K & k \\ -k & K \end{bmatrix} \begin{Bmatrix} \delta X \\ \delta Y \end{Bmatrix} + \begin{bmatrix} C & c \\ -c & C \end{bmatrix} \begin{Bmatrix} \delta \dot{X} \\ \delta \dot{Y} \end{Bmatrix}, \quad (1)$$

where δX and δY define rotor relative position, F_X and F_Y are the reaction-force components acting on the rotor, and K , k , C , c , are the direct and cross-coupled stiffness and damping coefficients, respectively. The second linearized model is for small motion about an arbitrary position within the seal and is stated

$$-\begin{Bmatrix} F_X \\ F_Y \end{Bmatrix} = \begin{bmatrix} K_{XX}(\epsilon_o) & K_{XY}(\epsilon_o) \\ K_{YX}(\epsilon_o) & K_{YY}(\epsilon_o) \end{bmatrix} \begin{Bmatrix} \delta X \\ \delta Y \end{Bmatrix} + \begin{bmatrix} C_{XX}(\epsilon_o) & C_{XY}(\epsilon_o) \\ C_{YX}(\epsilon_o) & C_{YY}(\epsilon_o) \end{bmatrix} \begin{Bmatrix} \delta \dot{X} \\ \delta \dot{Y} \end{Bmatrix} \quad (2)$$

where K_{XX} , K_{YY} , C_{XX} , C_{YY} , and K_{YX} , K_{XY} , C_{YX} , C_{XY} are the direct and cross-coupled stiffness and damping coefficients, respectively. These coefficients are functions of the static eccentricity ratio,

$$\epsilon_o = \frac{e_o}{C_r} \quad (3)$$

¹The research results reported here were supported in part by NASA Lewis Research Center through NASA grant NAG3-181; Technical Monitor, Robert C. Hendricks.

Contributed by the Tribology Division of THE AMERICAN SOCIETY OF MECHANICAL ENGINEERS and presented at the ASME/STLE Tribology Conference, Maui, Hawaii, October 16-19, 1994. Manuscript received by the Tribology Division February 7, 1994; revised manuscript received June 17, 1994. Paper No. 94-Trib-24. Associate Technical Editor: R. F. Salant.

where e_o is the static rotor displacement, and C_r is the centered radial clearance within the seal.

The model of Eq. (1) is clearly simpler than that of Eq. (2) and is normally used in rotordynamic analysis. Measurements of direct and cross-coupled stiffness coefficients by Benckert and Wachter (1980a,b) and Leong and Brown (1984) have confirmed the constant, eccentricity-independent, model of Eq. (1) for stiffness coefficients of labyrinth seals. For smooth annular seals, the present tests answer the question: For what magnitudes of e_o does the eccentricity-independent model of Eq. (1) remain valid?

The whirl frequency ratio f_w is a quantitative measure of rotordynamic instability and is defined using the eccentricity-dependent definition of Lund (1965):

$$f_w^2 = \frac{(K_{eq} - K_{XX})(K_{eq} - K_{YY}) - K_{XY}K_{YX}}{(C_{XX}C_{YY} - C_{XY}C_{YX})\omega^2}, \text{ where} \quad (4)$$

$$K_{eq} = \frac{K_{XX}C_{YY} + K_{YY}C_{XX} - C_{YX}K_{XY} - C_{XY}K_{YX}}{C_{XX} + C_{YY}},$$

and ω is the angular velocity of the rotor. The speed at which the tangential force becomes destabilizing is approximately

$$\omega_s = \frac{\omega_{nl}}{f_w}, \quad (5)$$

where ω_{nl} is the rotor's first critical speed and f_w is the whirl frequency ratio. As with hydrodynamic bearings, f_w for a long annular seals is about 0.5; hence, the seal will become destabilizing at a speed which is about twice the rotor's first critical speed. The question of interest here is: What influence does eccentric operation have on the rotordynamic coefficients, and, more specifically, how does eccentric operation influence stability as measured by the whirl-frequency ratio?

Gas Seal Theory

The bulk-flow analysis by Yang (1993) is used to solve for the rotordynamic and leakage characteristics of a smooth gas seal assuming compressible flow. The fluid is confined between the stator and the rotor where the fluid flow is governed by the continuity, momentum, and energy equations. Isothermal rotor and stator surfaces are assumed. Expansion of the governing equations yields zeroth and first order equations. Integration of the zeroth-order equations yields the pressure and leakage rates; whereas, integration of the first-order equations yields the rotordynamic coefficients.

Input data required for a computer code based on Yang's analysis are presented in Table 1 for the test seal configuration. The data in this table are for the lowest inlet pressure, back pressure, and speed, no inlet fluid prerotation, and the centered position. All values except those pertaining to the Moody friction factor can be obtained from experimental results. An entrance loss coefficient was selected as 0.5 based on the success of Kleynhans (1991). The smooth rotor and stator roughnesses were chosen as $8.128 \text{ E-}07 \text{ m}$ in accordance with the machined specifications and measurements.

Nomenclature

C, C_{XX}, C_{YY} = direct damping (N-s/mm)
 c, C_{YX}, C_{XY} = cross-coupled damping (N-s/mm)
 C_r = nominal radial seal clearance (mm)
 e_o = static rotor displacement (mm)
 F_X, F_Y = components of seal reaction (N)

K, K_{XX}, K_{YY} = direct stiffness coefficients (N/mm)
 k, K_{YX}, K_{XY} = cross-coupled stiffness coefficients (N/mm)
 P_b = back (sump) pressure (bars)
 P_r = inlet (reservoir) pressure (bars)
 P_{ra} = pressure ratio (P_b/P_r)

R = rotor radius (m)
 $\delta X, \delta Y$ = rotor-to-stator relative deflection at a seal
 e_o = static eccentricity ratio
 μ = fluid viscosity (N-s/m²)
 ρ = fluid density (kg/m³)
 ω = rotor angular velocity (rad/s)

Table 1 Input parameters for nominal values

Input parameter	Value
Seal clearance (inlet)	.41 mm
Seal clearance (exit)	.41 mm
Seal diameter	152 mm
Seal length	50.8 mm
Static rotor eccentricity, ϵ_{xo}	0.0
Static rotor eccentricity, ϵ_{yo}	0.0
Viscosity (reservoir)	$1.85 \times 10^{-5} \text{ N-s/m}^2$
Density (reservoir)	9.175 kg/m^3
Viscosity (sump)	$1.85 \times 10^{-5} \text{ N-s/m}^2$
Density (sump)	6.305 kg/m^3
Rotor speed	5000.0 rpm
Absolute pressure (reservoir)	7.918 bars
Absolute pressure (sump)	5.441 bars
Entrance loss coefficient	0.5
Preswirl factor, $U_{\theta o}/R\omega$	0.0
Relative roughness of rotor	0.001
Relative roughness of stator	0.001
Temperature (ambient)	300.7 K

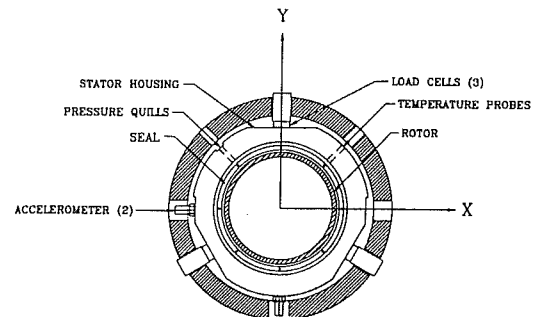


Fig. 1 Front view of test section

Apparatus and Testing

A thorough description of the test facility is provided by Childs et al. (1986), with the most recent modifications discussed in the work of Pelletti and Childs (1991). The facility uses air as the test fluid and allows for static vertical positioning of the rotor and static and dynamic control in the horizontal direction. Although the test apparatus only allows dynamic motion in the horizontal direction, independent identification of all eight rotordynamic coefficients can be performed by excitation parallel to the static eccentricity vector in the horizontal position and perpendicular to the static eccentricity vector in the vertical position. Excitation to identify $K_{XX}(\epsilon_o)$, $K_{YX}(\epsilon_o)$, $C_{XX}(\epsilon_o)$, and $C_{YX}(\epsilon_o)$ is performed at the static position ($C_r\epsilon_o, 0$) with horizontal motion parallel to the static eccentricity vector. In this case, rotor motion along the X axis causes a direct change in the clearance between the rotor and stator in the direction of excitation. Excitation to identify $K_{XY}(\epsilon_o)$, $K_{YY}(\epsilon_o)$, $C_{XY}(\epsilon_o)$, and $C_{YY}(\epsilon_o)$ is performed for the static position ($0, C_r\epsilon_o$) with horizontal excitation perpendicular to the static eccentricity vector. Rotor motion in this case does not

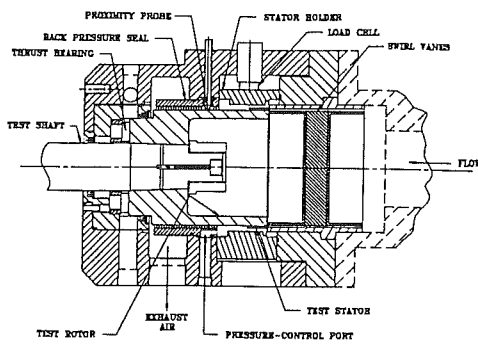


Fig. 2 Testing apparatus cross-sectional view

Table 2 Test points per static eccentricity ratio, ϵ_{x0} and ϵ_{y0}

Rotor speed (rpm) ω	Inlet pressure (bars) P_r	Pressure ratio (-) P_{ra}	Inlet preswirl in the direction of rotation
5,000	7.90	0.67	None
16,000	11.4	0.55	Intermediate
	14.8	0.50	High
		0.45	

cause a change in the minimum and maximum clearance and is moving parallel to the stator wall at the minimum and maximum clearance locations.

A front view of the test section including the seal geometry is shown in Fig. 1. The rotor is placed at a specified eccentric position within the seal where it is excited horizontally by pseudo random excitation forces via a hydraulic shaker head. The test seal stator is supported by three piezoelectric load cells which measure the test-seal reaction forces only. The motion and the reaction-force components exerted on the stator by the fluid are measured so that a hardware/software system can be used to identify all eight rotordynamic coefficients. A thorough description of this excitation process is provided by Childs and Hale (1994).

Figure 2 illustrates the test cross-section and identifies system components. Flow enters from the right and precedes through a set of preswirl vanes and the test seal before exiting through either the pressure-control port or across the back-pressure seal. Flow can be either withdrawn or injected from the pressure-control port to control the pressure ratio across the seal independently from the supply pressure. Note in Fig. 2 that only the test-seal stator forces are transmitted to the load cells.

Five independent test parameters were used, and the test matrix for each eccentric position is shown in Table 2. The inlet preswirl is in the direction of rotation and is the ratio of the fluid inlet circumferential velocity to the rotor surface velocity. The pressure ratio is defined as the absolute back pressure divided by the absolute inlet pressure and is varied independently from the inlet pressure.

Theory Versus Experiment

The experimental and theoretical rotordynamic characteristics for a smooth seal at eccentric operation will be compared. Results are presented to show the effects of inlet pressure (7.9, 11.4, and 14.8 bar), pressure ratio across the seal (0.67, 0.55, 0.50, 0.45), running speed (5,000 and 16,000 rpm), and inlet fluid prerotation (none, intermediate, and high). Results are presented in this section for direct stiffness K_{XX} , cross-coupled stiffness K_{YX} , direct damping C_{XX} , and the whirl frequency ratio. The leakage rate was invariant to changes in eccentricity for all operating conditions and will not be discussed. Data for cross-coupled damping are also not presented because the values are generally of the same order of magnitude as the uncertainty.

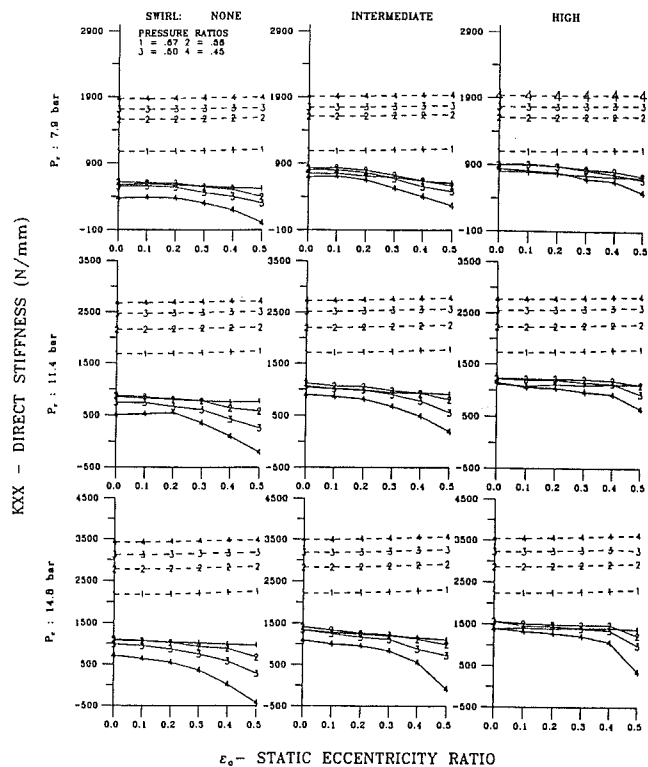


Fig. 3 Experimental (solid) versus theoretical (dashed) results for direct stiffness, K_{XX} , as a function of the static eccentricity ratio, ϵ_o , for a smooth seal at 16,000 rpm

Uncertainty Predictions. The analysis used to calculate the experimental uncertainty is based on the Kline-McClintock method as discussed and presented by Holman (1989). The calculations are based on the known uncertainties of the measuring equipment. The average uncertainty in the direct stiffness coefficients K_{XX} and K_{YY} , are 25.18 N/mm (2.86 percent) and 32.74 N/mm (2.86 percent), respectively. The cross-coupled stiffness uncertainties are 24.74 N/mm (2.99 percent) for K_{YX} and 21.42 (3.78 percent) for K_{XY} . The uncertainty values for direct damping, C_{XX} and C_{YY} , are 0.0461 N-s/mm (1.88 percent) and 0.061 N-s/mm (2.58 percent), respectively.

Direct Stiffness. Figure 3 shows K_{XX} as a function of the static eccentricity ratio ϵ_o at 16,000 rpm. Note that K_{XX} decreases with increasing eccentricity and increasing inlet pressure. The results obtained for K_{XX} at 5,000 rpm are similar except that the decrease in stiffness at higher eccentricities was not as significant. The direct stiffness K_{YY} does not change significantly with increasing eccentricity at either of the tested speeds. This is because identification of K_{XX} requires excitation directly towards the stator wall, while identification of K_{YY} uses motion which is nominally parallel to the wall. For the same reason, C_{XX} and K_{YX} change more significantly with eccentricity than C_{YY} and K_{XY} , respectively.

With regards to K_{XX} , the theoretical predictions are inaccurate in several regards. The analytical results overpredict direct stiffness for all conditions and also incorrectly indicate increasing stiffness with decreasing pressure ratios. Predictions also fail to indicate that increasing eccentricity causes a notable decrease in the direct stiffness values.

Cross-Coupled Stiffness. K_{YX} is presented as a function of ϵ_o at 16,000 rpm in Fig. 4. As discussed previously, K_{YX} does not change significantly with eccentricity and is not presented. Theory correctly indicates increasing values of K_{YX} for increases in inlet preswirl, inlet pressure, speed, and the static eccentricity ratio. At 5,000 rpm K_{YX} also increases with increasing eccentricity (although less than at 16,000 rpm) which

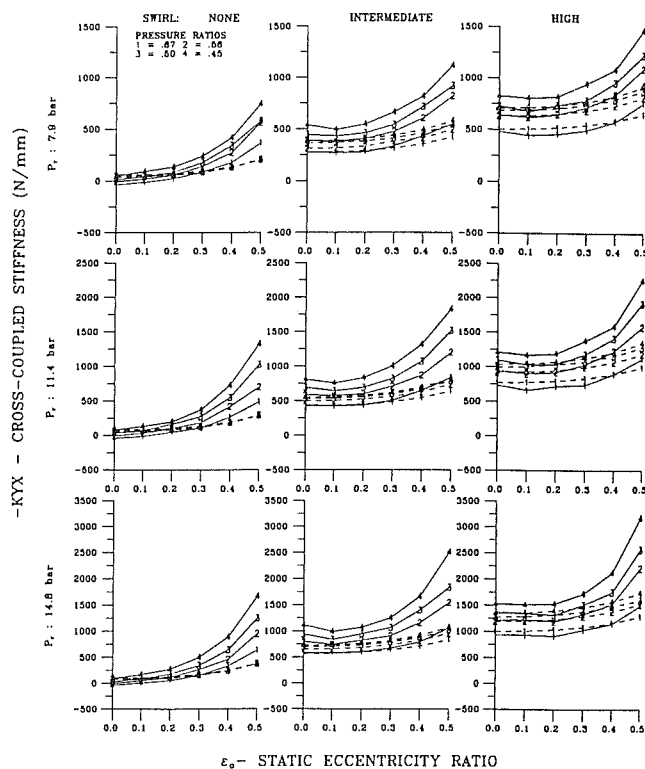


Fig. 4 Experimental (solid) versus theoretical (dashed) results for cross-coupled stiffness, K_{YX} , as a function of the static eccentricity ratio, ϵ_o , for a smooth seal at 16,000 rpm

is correctly shown by theory. Overall, the results show good agreement between theory and measurements, although K_{YX} measurements consistently increase more rapidly with increasing eccentricity than predicted.

Direct Damping. Figure 5 shows C_{XX} as a function of ϵ_o at 16,000 rpm. Direct damping increases with increasing eccentricity. This trend also held at 5000 rpm but to a less significant degree. Both experimental and theoretical results for C_{XX} increase with increasing eccentricity. Theory underpredicts the increase in direct damping that occurs with increasing eccentricity and fails to indicate that increasing inlet preswirl reduces the direct damping values. The theory correctly predicts an increase in C_{XX} with decreasing pressure ratio. Correlation between theory and experiment is worst at low supply pressure and low preswirl and improves steadily as either preswirl or supply pressure is increased.

Whirl Frequency Ratio. The whirl frequency ratio is shown in Fig. 6 as a function of the static eccentricity ratio ϵ_o at 5000 rpm. With no swirl, the results closely match theory because neither theory or prediction change significantly with eccentricity. With preswirl, theoretical and experimental results differ. Theory predicts a slight decrease in the whirl frequency ratio, but the experimental results show f_w increasing with increasing eccentricity. Although the experimental and analytical results differ considerably at the centered position, they converge to comparable values at higher eccentricities. The experimental and theoretical results at 16,000 rpm do not change with increasing eccentricity. This outcome indicates that at higher speeds, stability is not altered with changes in eccentricity; whereas, at lower speeds, increasing eccentricity decreases stability for preswirl flow.

Discussion and Conclusion

Tests results show that changes in ϵ_o have a significant effect

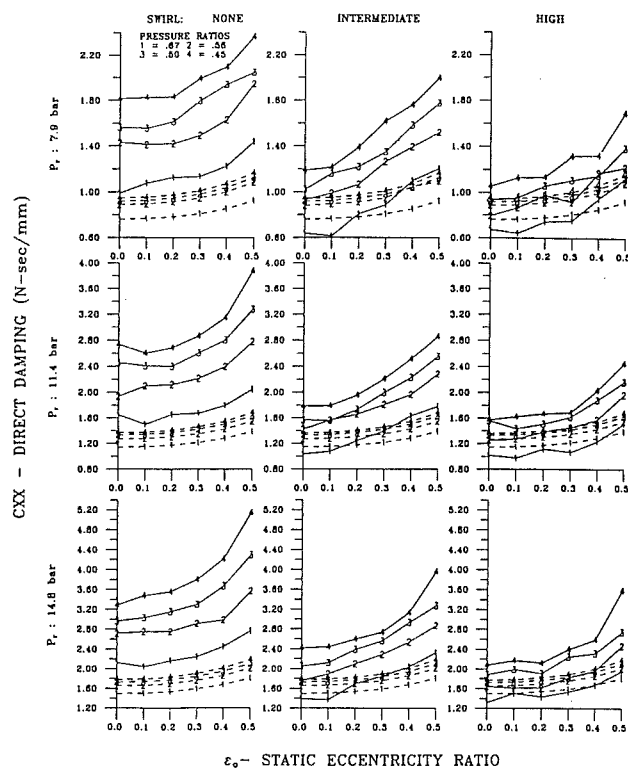


Fig. 5 Experimental (solid) versus theoretical (dashed) results for direct damping, C_{XX} , as a function of the static eccentricity ratio, ϵ_o , for a smooth seal at 16,000 rpm

on the rotordynamic characteristics of a smooth gas seal. The simple eccentricity-independent model of Eq. (1) is only valid out to comparatively small eccentricities on the order of 0.2~0.3. For larger eccentricity values, the eccentricity-dependent model of Eq. (2) should be used.

The decrease in the direct stiffness that occurs with increasing eccentricity is significant when considering seal configurations which depend on direct stiffness to center the seal stator relative to the displaced rotor, e.g., floating-ring seals. The theoretical results fail to show the decrease that occurs with increasing eccentricity. The experimental and theoretical results both show that cross-coupled stiffness increases with increasing eccentricity, although the theory fails to indicate the marked increase that occurs with eccentricity ratios greater than 0.2.

The theory significantly underestimates direct damping at low supply pressures and low preswirl with a steady improvement as either of these parameters is increased. Direct damping increases with increasing eccentricity, which is correctly predicted by theory.

Concerning rotor dynamic stability as measured by the whirl-frequency ratio f_w , at 5000 rpm, for preswirl flow, stability decreases with increasing eccentricity. For flow with no preswirl, the whirl-frequency ratio was near zero and did not change with increasing ϵ_o . At 16,000 rpm, f_w was insensitive to operating eccentricity.

Although not illustrated here, out to an eccentricity ratio of 0.5 both theory and experiment showed no changes in the mass flow rate due to a change in eccentricity. Predictions of leakage were in good agreement with measurements in all cases.

Yang's (1993) analysis provides reasonable predictions for all the rotordynamic coefficients (excluding direct stiffness and direct damping at low supply pressures and low preswirl) as well as the leakage and pressure profile characteristics. The code is effective in predicting the trends associated with the performance characteristics of a smooth seal, although it does not show the sensitivity to variations in the pressure ratios found in the experimental results.

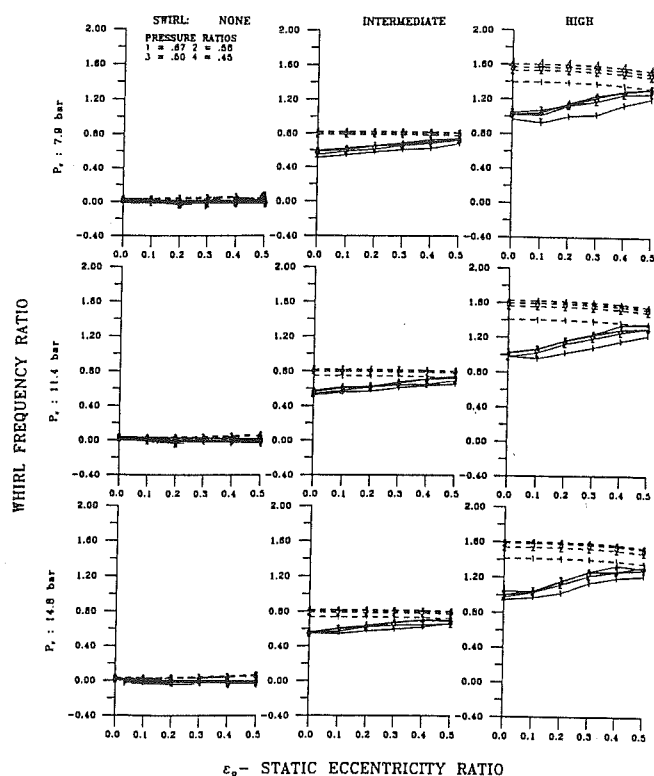


Fig. 6 Experimental (solid) versus theoretical (dashed) results for whirl frequency ratio as a function of the static eccentricity ratio, ϵ_0 , for a smooth seal at 5000 rpm

Most operating turbomachines have seals which operate eccentrically. This research indicates that rotordynamic coefficients are sensitive to changes in the static eccentricity ratio for all speeds, although the highest operating eccentricity of

this research was only 0.5. Continued investigations are needed to study the effects of eccentricity on the rotordynamic and leakage characteristics of other seal configurations.

References

- Alexander, C. R., 1993, "Comparison of Theoretical and Experimental Rotordynamic Coefficients for a Smooth Seal at Eccentric Operation," M.S. thesis, Texas A&M University.
- Benckert, H., and Wachter, J., 1980a, "Flow Induced Spring Coefficients of Labyrinth Seals for Applications in Turbomachinery," NASA CP 2133, Rotordynamic Instability Problems in High-Performance Turbomachinery, Proceedings of a Workshop held at Texas A&M University by the Turbomachinery Laboratory, pp. 189-212.
- Benckert, H., and Wachter, J., 1980b, "Flow Induced Spring Constants of Labyrinth Seals," Proceedings, *IMEchE of the 2nd International Conference on Vibrations in Rotating Machinery*, pp. 56-63.
- Childs, D. W., Nelson, C. C., Nicks, C., Scharrer, J., Elrod, D., and Hale, K., 1986, "Theory Versus Experiment for the Rotordynamic Coefficients of Annular Gas Seals: Part I—Test Facility and Apparatus," *ASME JOURNAL OF TRIBOLOGY*, Vol. 108, pp. 426-432.
- Childs, D. W., 1993, *Turbomachinery Rotordynamics*, John Wiley & Sons, New York, pp. 164, 173, 290-294.
- Childs, D. W., and Hale, K., 1994, "A Test Apparatus and Facility to Identify the Rotordynamic Coefficients of High-Speed Hydrostatic Bearings," *ASME JOURNAL OF TRIBOLOGY*, Vol. 116, pp. 337-344.
- Holman, J. P., 1989, *Experimental Methods for Engineers*, McGraw-Hill, New York, pp. 41-42.
- Kleynhans, G. F., 1991, "A Comparison of Experimental Results and Theoretical Predictions for the Rotordynamic and Leakage Characteristics of Short ($L/D = 1/6$) Honeycomb and Smooth Annular Pressure Seals," M.S. thesis, Texas A&M University.
- Leong, Y., and Brown, D., 1984, "Experimental Investigation of Lateral Forces Induced by Flow Through Model Labyrinth Seals," NASA CP 2338, Rotordynamic Instability Problems in High-Performance Turbomachinery, pp. 187-210.
- Lund, J., 1965, "The Stability of an Elastic Rotor in Journal Bearings with Flexible, Damped Supports," *ASME Journal of Applied Mechanics*, pp. 911-920.
- Pelletti, J. M., and Childs, D. W., 1991, "A Comparison of Experimental Results and Theoretical Predictions for the Rotordynamic Coefficients of Short ($L/D = 1/6$) Labyrinth Seals," *Proceedings, 1991 ASME Design Technical Conference*, DE-Vol. 35, pp. 69-76.
- Yang, Z., 1993, "Dynamic Force Performance of Annular Gas Seals at Off-Center Conditions," STLE Paper 93-AM-4D-1.

Published Quarterly by The American Society of Mechanical Engineers

VOLUME 117 • NUMBER 1 • JANUARY 1995

Technical Editor,
F. E. KENNEDY, JR.

Associate Technical Editors

M. J. BRAUN (1997)

D. E. BREWE (1996)

C. CUSANO (1996)

J. ETSION (1997)

T. FARRIS (1997)

S. IOANNIDES (1995)

K. KATO (1996)

K. KOMVOPOULOS (1995)

A. K. MENON (1996)

R. F. SALANT (1996)

P. SUTOR (1997)

K. TONDER (1997)

Past Technical Editors

D. F. WILCOCK (1967-1974)

D. F. HAYS (1975-1980)

W. O. WINER (1981-1987)

A. Z. SZERI (1988-1993)

TRIBOLOGY DIVISION

Chairman, F. E. KENNEDY, JR.

Secretary, D. B. BOGY

BOARD ON COMMUNICATIONS

Chairman and Vice President

R. D. ROCKE

Members-at-Large

J. BARLOW, N. H. CHAO, A. ERDMAN,

G. JOHNSON, L. KEER, W. MORGAN,

PATTON, S. PATULSKI, R. E. REDER,

S. ROHDE, R. SHAH, F. WHITE,

J. WHITEHEAD

OFFICERS OF THE ASME

President, P. J. TORPEY

Exec. Director

D. L. BELDEN

Treasurer

R. A. BENNETT

PUBLISHING STAFF

Mng. Dir. Publ.

CHARLES W. BEARDSLEY

Managing Editor

CORNELIA MONAHAN

Production Assistant

MARISOL ANDINO

Transactions of the ASME, Journal of Tribology (ISSN 0742-4787) is published quarterly (Jan., April, July, Oct.) for \$150.00 per year by The American Society of Mechanical Engineers, 345 East 57th Street, New York, NY 10022. Second class postage paid at New York, NY and additional mailing offices. POSTMASTER: Send address changes to Transactions of the ASME, Journal of Tribology, THE AMERICAN SOCIETY OF MECHANICAL ENGINEERS, 22 Law Drive, Box 2300, Fairfield, NJ 07007-2300.

CHANGES OF ADDRESS must be received at Society headquarters seven weeks before they are to be effective. Please send old label and new address. PRICES: To members, \$40.00 annually; to nonmembers, \$150.00. Add \$30.00 for postage to countries outside the United States and Canada.

STATEMENT from By-Laws: The Society shall not be responsible for statements or opinions advanced in papers or printed in its publications (B7.1, Par. 3). COPYRIGHT © 1995 by The American Society of Mechanical Engineers. Authorization to photocopy material for internal or personal use under circumstances not falling within the fair use provisions of the Copyright Act is granted by ASME to libraries and other users registered with the Copyright Clearance Center (CCC) Transactional Reporting Service provided that the base fee of \$3.00 per article is paid directly to CCC, 222 Rosewood Drive, Danvers, MA 01923. Request for special permission or bulk copying should be addressed to Reprints/Permission Department.

INDEXED by Applied Mechanics Reviews and Engineering Information, Inc. Canadian Goods & Services Tax Registration #120140543

- 1 Polymer/Metal Conformal Sliding Contact With Forced Convection Cooling (94-Trib-1)
J. K. Haverstick and T. C. Ovaert
- 9 Asymptotic Analysis of Ultra-Thin Gas Squeeze Film Lubrication for Infinitely Large Squeeze Number (Extension of Pan's Theory to the Molecular Gas Film Lubrication Equation) (94-Trib-2)
R. Matsuda and S. Fukui
- 16 A Porous Media Model for Thin Film Lubrication (94-Trib-3)
J. A. Tichy
- 22 Rheological Models for Thin Film EHL Contacts (94-Trib-4)
Siyoul Jang and John Tichy
- 29 Fundamental Differences Between Newtonian and Non-Newtonian Micro-EHL Results (94-Trib-5)
L. Chang and W. Zhao
- 36 A Numerical Scheme for Static and Dynamic Simulation of Subambient Pressure Shaped Rail Sliders (94-Trib-6)
Ellis Cha and D. B. Bogy
- 47 The Slippery Sheet (94-Trib-7)
R. C. Benson
- 53 Elastohydrodynamic Analysis of Reverse Pumping in Rotary Lip Seals With Microasperities (94-Trib-9)
Richard F. Salant and Andrew L. Flaherty
- 60 Evaluating Surface Roughness From Contact Vibrations (94-Trib-10)
Daniel P. Hess and Nitish J. Wagh
- 65 Boric Acid as an Additive for Core-Drilling of Alumina (94-Trib-11)
H. Liang and S. Jahanmir
- 74 Oil Drop Formation at the Outlet of an Elastohydrodynamic Lubricated Point Contact (94-Trib-12)
Per-Olof Larsson, Bo Jacobson, and Erik Höglund
- 80 Mixed Lubrication Characteristics Between the Piston and Cylinder in Hydraulic Piston Pump-Motor (94-Trib-13)
Yi Fang and Masataka Shirakashi
- 86 Slider Overcoats for Enhanced Interface Durability in Magnetic Recording Applications (94-Trib-14)
S. K. Ganapathi and Timothy A. Riener
- 94 Numerical Simulation of a Ball Impacting and Rebounding a Lubricated Surface (94-Trib-15)
Roland Larsson and Erik Höglund
- 103 Theoretical Analysis of Externally Pressurized Porous Foil Bearings—Part I: In the Case of Smooth Surface Porous Shaft (94-Trib-17)
H. Hashimoto
- 112 Optical Surface Analysis of the Head-Disk-Interface of Thin Film Disks (94-Trib-18)
Steven W. Meeks, Walter E. Weresin, and Hal J. Rosen
- 119 Slider/Disk Interaction During the Landing Process (94-Trib-19)
H.-Leo, S. R. Chapman, and R. M. Crone
- 124 Computer Analysis of the Dynamic Contact Behavior and Tracking Characteristics of a Single-Degree-of-Freedom Slider Model for a Contact Recording Head (94-Trib-20)
Kyosuke Ono, Hiroshi Yamamura, and Takaaki Mizokashi
- 130 Physical Modeling and Data Analysis of the Dynamic Response of a Flexibly Mounted Rotor Mechanical Seal (94-Trib-21)
An Sung Lee and Itzhak Green
- 136 A Finite Element Scheme for Determining the Shaped Rail Slider Flying Characteristics With Experimental Confirmation (94-Trib-22)
Jih-Ping Peng and Cal E. Hardie
- 143 Improved Design With Noncylindrical Profiles of Gas-Lubricated Ringless Pistons (94-Trib-23)
I. Etsion and K. Gomed

(Contents continued on page 15)

Intro

The
has b
many
wides
beari
tages.
signif
plasti
tively
condu
rapid.
theref
suitab
uration
Mo
specifi
at high
refer to
pair is
condit
arise f
and si
It is w
wear o
dissipa
sliding

Contri
CHANICAL
Maui, H
Division
No. 94-T

Journal